THE JOURNAL OF PHYSICAL CHEMISTRY Letters

Letter

Cite This: J. Phys. Chem. Lett. 2018, 9, 2367−2372

pubs.acs.org/JPCL

On-the-Fly Ab Initio Semiclassical Evaluation of Absorption Spectra of Polyatomic Molecules beyond the Condon Approximation

Aurélien Patoz,[†] Tomislav Begušić,[†] and Jiří Vaníček*

Laboratory of Theoretical Physical Chemistry, Institut des Sciences et Ingénierie Chimiques, Ecole Polytechnique Fédérale de Lausanne (EPFL), CH-1015 Lausanne, Switzerland

Supporting Information

ABSTRACT: To evaluate vibronic spectra beyond the Condon approximation, we extend the on-the-fly ab initio thawed Gaussian approximation by considering the Herzberg−Teller contribution due to the dependence of the electronic transition dipole moment on nuclear coordinates. The extended thawed Gaussian approximation is tested on electronic absorption spectra of the phenyl radical and benzene; calculated spectra reproduce experimental data and are much more accurate than standard global harmonic approaches, confirming the significance of anharmonicity. Moreover, the extended method provides a tool to quantify the Herzberg−Teller contribution; we show that in the phenyl radical, anharmonicity outweighs the Herzberg−Teller contribution, whereas in benzene, the Herzberg−Teller contribution is essential because the transition is electronically forbidden and the Condon approximation yields a zero spectrum. Surprisingly, both adiabatic harmonic spectra outperform those of the vertical harmonic model, which describes the Franck−Condon region better. Finally, we provide a simple recipe for orientationally averaging spectra, valid beyond the Condon approximation, and a relation among the transition dipole, its gradient, and nonadiabatic coupling vectors.

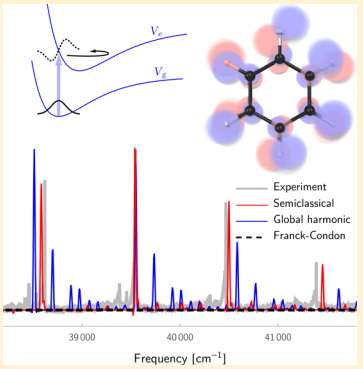

Vibrationally resolved electronic spectroscopy provides valuable insight into the structure and dynamics of polyatomic molecules.[1] Indeed, light-induced molecular dynamics is recognized as one of the key areas of research in physical chemistry, not only for fundamental understanding of nature but also for various applications, from solar cells to photodynamic therapy.[2] The development of theoretical methods for simulating and understanding optical spectra is, therefore, of great importance.

The time-dependent approach to spectroscopy[3] evaluates the vibronic spectrum as the Fourier transform of the nuclear wavepacket autocorrelation function and, in contrast to the commonly used time-independent Franck−Condon (FC) approach,[4,5] can easily account for effects beyond the Born−Oppenheimer and global harmonic approximations. In the time-dependent approach, one must first perform exact or approximate molecular quantum dynamics. While exact quantum dynamics typically requires a global potential energy surface[6,7] and scales exponentially with dimensions, semiclassical methods, such as the initial value representation,[8] thawed Gaussian approximation (TGA),[9] frozen Gaussian approximation,[10] and Herman−Kluk propagator[11,12] require only local information and are suitable for on-the-fly implementation. The idea of using multiple frozen Gaussians as a basis for describing the full wavepacket has inspired a number of quantum[13−15] and semiclassical[16−21] "first-principles" approaches, which allow combination with an on-the-fly ab initio (OTF-AI) evaluation of the electronic structure. Apart from a few examples,[22] thawed Gaussians have been largely marginalized because they can describe neither wavepacket splitting nor very anharmonic dynamics. Yet, vibrationally resolved electronic spectra are mostly determined by short-time dynamics, during which both wavepacket splitting and anharmonic effects are less important. Indeed, a recent implementation of OTF-AI-TGA reproduced successfully the vibrational structure of electronic absorption, emission, and photoelectron spectra, even in rather anharmonic and floppy systems such as ammonia.[23,24]

Here, an extension of the OTF-AI-TGA beyond the Condon approximation is presented by employing the Herzberg−Teller (HT) approximation,[25] which, in contrast to the Condon approximation,[4] includes a linear dependence of the transition dipole moment on nuclear coordinates. We employ OTF-AI implementation of the extended thawed Gaussian approximation (ETGA)[26] to evaluate the absorption spectra of the phenyl radical, an anharmonic system allegedly exhibiting a significant HT contribution,[27] and benzene, a textbook example of a symmetry-forbidden (i.e., electronically forbidden) transition.[28]

At zero temperature, within the electric dipole approximation, first-order time-dependent perturbation theory, and rotating-wave approximation, the absorption cross section of a molecule with two electronic states that are not nonadiabatically coupled can be expressed as the Fourier transform

Received: March 16, 2018
Accepted: April 13, 2018
Published: April 13, 2018

DOI: 10.1021/acs.jpclett.8b00827
J. Phys. Chem. Lett. 2018, 9, 2367−2372

$$\sigma_{\mu\mu}(\omega) = \frac{2\pi\omega}{\hbar c}\int_{-\infty}^{\infty} C_{\mu\mu}(t)\mathrm{e}^{\mathrm{i}\omega t}\,\mathrm{d}t \tag{1}$$

of the dipole time autocorrelation function

$$\begin{aligned} C_{\mu\mu}(t) &= \langle 1,\mathrm{g} \mid \mathrm{e}^{\mathrm{i}\hat{H}_1 t/\hbar}\hat{\mu}^{*}\mathrm{e}^{-\mathrm{i}\hat{H}_2 t/\hbar}\hat{\mu} \mid 1,\mathrm{g}\rangle \\ &= \langle \phi(0) \mid \phi(t)\rangle \mathrm{e}^{-\mathrm{i}E_{1,\mathrm{g}}t/\hbar} \end{aligned} \tag{2}$$

where $\hat{H}_1$ and $\hat{H}_2$ are nuclear Hamiltonian operators of the ground and excited electronic states, $\hat{\mu}$ is the matrix element $\hat{\vec{\mu}}_{21}$ of the electric transition dipole moment operator projected along the polarization unit vector $\vec{\epsilon}$, i.e., $\hat{\mu} := \hat{\vec{\mu}}_{21}\cdot\vec{\epsilon}$ (the subscript 21 is removed for simplicity because we will almost exclusively consider this matrix element), and $|1,\mathrm{g}\rangle$ is the ground vibrational state of the ground electronic state with zero-point energy $E_{1,\mathrm{g}}$. Thus, the vibronic spectrum can be evaluated by propagating the initial wavepacket $|\phi(0)\rangle = \hat{\mu}|1,\mathrm{g}\rangle$ on the excited-state potential energy surface.

To compare with an experiment in the gas phase, where the molecules are isotropically distributed, one must average the computed spectrum over all molecular orientations. Yet, due to the isotropy of space, brute-force numerical averaging is avoided; averaging is required only over three orientations of the molecule.[29] To show this, consider the spectrum and autocorrelation function as 3×3 tensors $\sigma_{\vec{\mu}\vec{\mu}}(\omega)$ and $C_{\vec{\mu}\vec{\mu}}(t)$, the latter related to $C_{\mu\mu}(t)$ by $C_{\mu\mu}(t) = \vec{\epsilon}^{\mathrm{T}}\cdot C_{\vec{\mu}\vec{\mu}}(t)\cdot\vec{\epsilon}$. A simple analytical calculation[30] shows that the average over all orientations of the polarization vector $\vec{\epsilon}$ is $\overline{C_{\mu\mu}(t)} = \frac{1}{3}\mathrm{Tr}[C_{\vec{\mu}\vec{\mu}}(t)]$ and the corresponding absorption cross section is

$$\overline{\sigma(\omega)} = \frac{1}{3}\mathrm{Tr}[\sigma_{\vec{\mu}\vec{\mu}}(\omega)] = \frac{1}{3}(\sigma_{\mu_x\mu_x} + \sigma_{\mu_y\mu_y} + \sigma_{\mu_z\mu_z}) \tag{3}$$

Thus, the average is easily evaluated, e.g., by averaging over only three arbitrary orthogonal molecular orientations with respect to the fixed polarization vector $\vec{\epsilon}$ or by fixing the molecular orientation and averaging over only three arbitrary orthogonal polarization vectors.

While the result (eq 3) holds for arbitrary coordinate dependence of the transition dipole $\vec{\mu}(q)$, two approximations are frequently used. Within the most common Condon approximation, the transition dipole is considered constant, $\vec{\mu}(q) \approx \vec{\mu}(q_0)$, and the general result (eq 3) reduces to the textbook recipe for the averaged spectrum, which we shall call the FC spectrum:

$$\overline{\sigma_{\mathrm{FC}}(\omega)} = \frac{1}{3}\sigma_{|\vec{\mu}||\vec{\mu}|}(\omega) \tag{4}$$

("Divide the spectrum for the molecular dipole aligned with the field by 3.") In the more accurate HT approximation, the transition dipole moment becomes a linear function of nuclear coordinates:

$$\vec{\mu}(q) \approx \vec{\mu}(q_0) + \mathrm{grad}_q\,\vec{\mu}|_{q_0}^{\mathrm{T}}\cdot(q - q_0) \tag{5}$$

By explicitly differentiating the matrix element $\vec{\mu}_{\alpha\beta}$ of the molecular dipole between electronic states α and β (for a moment, we reintroduce the subscripts), one can show[30] that

$$\frac{\partial}{\partial q_i}\vec{\mu}_{\alpha\beta} = \sum_{\gamma}(\vec{\mu}_{\alpha\gamma}F_{i,\gamma\beta} - F_{i,\alpha\gamma}\vec{\mu}_{\gamma\beta}) + \left(e\sum_{j=1}^{N} Z_j\frac{\partial\vec{R}_j}{\partial q_i}\right)\delta_{\alpha\beta} \tag{6}$$

or, in a more compact matrix notation

$$\frac{\partial}{\partial q_i}\vec{\boldsymbol{\mu}} = [\vec{\boldsymbol{\mu}}, \mathbf{F}_i] + \left(e\sum_{j=1}^{N} Z_j\frac{\partial\vec{R}_j}{\partial q_i}\right)\mathbf{1} \tag{7}$$

where N is the number of atoms, Z_j the atomic number, $\vec{R}_j$ the coordinates of the jth atom, and $F_{i,\alpha\beta} := \langle\alpha|(\partial\beta/\partial q_i)\rangle$ is the ith component of the nonadiabatic coupling vector between states α and β. For the *transition* dipole moment, $\alpha\neq\beta$ and the term proportional to $\delta_{\alpha\beta}$ in eq 6 (to $\mathbf{1}$ in eq 7) vanishes, which shows that the HT dependence originates from a combination of nonzero nonadiabatic and dipole couplings of states α and β to an intermediate state γ. Moreover, because one may usually neglect nonadiabatic couplings between the ground and excited electronic states at the ground-state optimized geometry, only the second term of the commutator survives:

$$\frac{\partial}{\partial q_j}\vec{\mu}_{21} \approx -\sum_{\gamma} F_{i,2\gamma}\vec{\mu}_{\gamma 1} \tag{8}$$

showing that a nonvanishing gradient of the transition dipole between the ground state 1 and excited state 2 requires an intermediate, "bright" ($\vec{\mu}_{\gamma 1}\neq 0$) excited state γ that is vibronically coupled ($F_{i,2\gamma}\neq 0$) to the excited state 2. Such interpretation reveals the deep connection between the HT approximation and the concepts of "vibronic coupling" and "intensity borrowing."[31] Finally, although eq 7 suggests a way to evaluate $\partial_q\vec{\mu}_{\alpha\beta}$ from $\vec{\boldsymbol{\mu}}$ and $\mathbf{F}_i$, it is usually easier to evaluate the gradient by finite difference.

To find the autocorrelation function $C_{\mu\mu}(t)$, one must propagate the wavepacket. Heller's TGA[3,9,26] relies on the fact that a Gaussian wavepacket evolved in at most a quadratic potential remains a Gaussian. Within this approximation, the anharmonicity of the potential is taken into account partially by propagating the Gaussian wavepacket

$$\begin{aligned} \psi_t(q) = N_0\exp\Big\{&-(q - q_t)^{\mathrm{T}}\cdot A_t\cdot(q - q_t) \\ &+ \frac{\mathrm{i}}{\hbar}[p_t^{\mathrm{T}}\cdot(q - q_t) + \gamma_t]\Big\} \end{aligned} \tag{9}$$

in the time-dependent effective potential given by the local harmonic approximation of the full potential:

$$\begin{aligned} V_{\mathrm{eff}}(q,t) = {}& V|_{q_t} + (\mathrm{grad}_q V|_{q_t})^{\mathrm{T}}\cdot(q - q_t) \\ &+ \frac{1}{2}(q - q_t)^{\mathrm{T}}\cdot\mathrm{Hess}_q V|_{q_t}\cdot(q - q_t) \end{aligned} \tag{10}$$

where $V|_{q_t}$, $\mathrm{grad}_q V|_{q_t}$, and $\mathrm{Hess}_q V|_{q_t}$ denote the potential energy, gradient, and Hessian evaluated at the center of the Gaussian, N_0 is the initial normalization constant, (q_t,p_t) are the phase-space coordinates of the center of the Gaussian wavepacket at time t, A_t is the complex symmetric width matrix, and γ_t is a complex number; its real part gives an overall phase factor, and its imaginary part ensures the normalization of the Gaussian wavepacket at all times. Parameters of the Gaussian follow Heller's equations of motion[3,9,26]

$$\dot{q}_t = m^{-1}\cdot p_t \tag{11}$$

$$\dot{p}_t = -\mathrm{grad}_q V|_{q_t} \tag{12}$$

DOI: 10.1021/acs.jpclett.8b00827
J. Phys. Chem. Lett. 2018, 9, 2367−2372

$$\dot{A}_t = -2i\hbar A_t \cdot m^{-1} \cdot A_t + \frac{i}{2\hbar} \mathrm{Hess}_q V|_{q_t} \tag{13}$$

$$\dot{\gamma}_t = L_t - \hbar^2 \mathrm{Tr}(m^{-1} \cdot A_t) \tag{14}$$

where m is the diagonal mass matrix and L_t the Lagrangian.

The extended TGA used in this work considers a more general form of the initial wavepacket, namely, a Gaussian wavepacket (eq 9) multiplied by a polynomial $P(q - q_0)$ in nuclear coordinates, which, at time zero, can be written as a polynomial in the derivatives with respect to p_0:

$$\phi_0(q) = P(q - q_0)\psi_0(q) = P\left(\frac{\hbar}{i}\frac{\partial}{\partial p_0}\right)\psi_0(q) \tag{15}$$

This observation leads to a simple recipe for propagating the extended TGA wavepacket within the local harmonic approximation,[26] namely, the wavepacket retains this form at all times:

$$\phi_t(q) = P\left(\frac{\hbar}{i}\frac{\partial}{\partial p_0}\right)\psi_t(q) \tag{16}$$

where $\psi_t(q)$ is the original TGA wavepacket (eq 9). As for the initial HT wavepacket, $P(q - q_0) = \mu(q_0) + b_0^{\mathrm{T}} \cdot (q - q_0)$, where $b_0 = \mathrm{grad}_q \mu|_{q_0}$, and the semiclassical propagation yields

$$\phi_t(q) = [\mu(q_0) + b_t^{\mathrm{T}} \cdot (q - q_t)]\psi_t(q) \tag{17}$$

The four parameters of the Gaussian $\psi_t(q)$ are propagated with the usual TGA eqs 11−14, and only one additional parameter, b_t, must be evaluated:

$$b_t = (-2i\hbar A_t \cdot M_{qp,t} + M_{pp,t}) \cdot b_0 \tag{18}$$

where $M_{qp,t} = \partial q_t/\partial p_0$ and $M_{pp,t} = \partial p_t/\partial p_0$ are the elements of the stability matrix, which is already needed to propagate A_t and γ_t, implying that the additional evaluation of b_t comes at almost no additional cost. Remarkably, the orientational averaging of ETGA spectra is even simpler than what could be expected from the general simplification that we mentioned in the beginning: within ETGA, the averaging requires only a single trajectory (instead of three) because the transition dipole moment does not affect the propagation of q_t, p_t, A_t, and γ_t.

As a consequence of this property, the ETGA can be combined with an OTF-AI scheme at the same cost as the original TGA for spectra within the Condon approximation.[23,24] The ab initio calculations are typically performed in Cartesian coordinates, and therefore, the ab initio gradients and Hessians needed in eq 10 must be transformed[23,24] to the coordinate system q that fits into our framework—the vibrational normal modes.

As the extended TGA is exact in a globally harmonic potential, it is useful to compare the on-the-fly approach with two common approximations of the excited-state potential energy surface, the vertical harmonic (VH) and adiabatic harmonic (AH) approximations,[32] in which the excited-state potential is expanded to second order about the ground- and excited-state optimized geometries, respectively (see refs 23 and 24 for details). We use density functional theory for the ground-state and time-dependent density functional theory for the excited-state ab initio calculations, employing B3LYP functional with SNSD basis set for the phenyl radical and B3LYP functional with 6-31+G(d,p) basis set for benzene (see the Supporting Information for details and validation by comparison with a higher-level ab initio method).

According to Barone and co-workers,[27,33] calculation of the absorption spectrum corresponding to $\tilde{A}^2B_1 \leftarrow \tilde{X}^2A_1$ electronic transition of the phenyl radical depends on the dimensionality of the simulation model and on inclusion of the HT contribution, anharmonicity effects, and mode mixing (Duschinsky effect).[34] Our model includes all of these effects and provides the means to evaluate their importance.

To assess the influence of anharmonicity, the experimental spectrum is compared with the spectra simulated using the global harmonic approaches (Figure 1, top). While the vertical

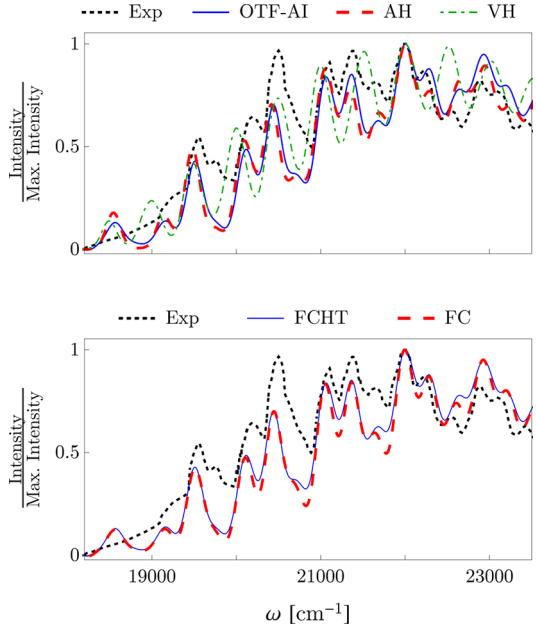

Figure 1. Calculated absorption spectra of the phenyl radical $\tilde{A}^2B_1 \leftarrow \tilde{X}^2A_1$ electronic transition compared to the experimental[33,38] spectrum measured in an Ar matrix at 6 K. Top: Comparison of the OTF-AI-ETGA, AH, and VH models (all three are the FCHT spectra, based on the HT approximation, eq 5). Bottom: Comparison of the FC and FCHT spectra (both evaluated with OTF-AI-ETGA). All spectra are horizontally shifted and rescaled according to the highest peak (see Table S7 of the Supporting Information).

harmonic approach only captures the overall envelope of the experimental spectrum but fails to capture any details, the AH model reproduces all main features of the spectrum. This is in contrast with the common expectation that the vertical harmonic approach should be more accurate[32,35] as it describes better the FC region of the excited-state potential. Indeed, the emission spectra of oligothiophenes[23] and both absorption and photoelectron spectra of ammonia[24] are much better described with the VH than the AH approach. In phenyl radical, the failure of the VH approach lies in the incorrect frequencies and displacements of the two most displaced modes 18 and 24 (Figure S4 of the Supporting Information), resulting in the missing mode effect:[36,37] when the spectrum is not well resolved, it may contain a single progression whose spacing does not correspond to any of the vibrational frequencies of the system. Unlike the global harmonic approaches, the on-the-fly method overcomes the problem of guessing which excited-state Hessian should be used (i.e., vertical or adiabatic) and

DOI: 10.1021/acs.jpclett.8b00827
J. Phys. Chem. Lett. 2018, 9, 2367−2372

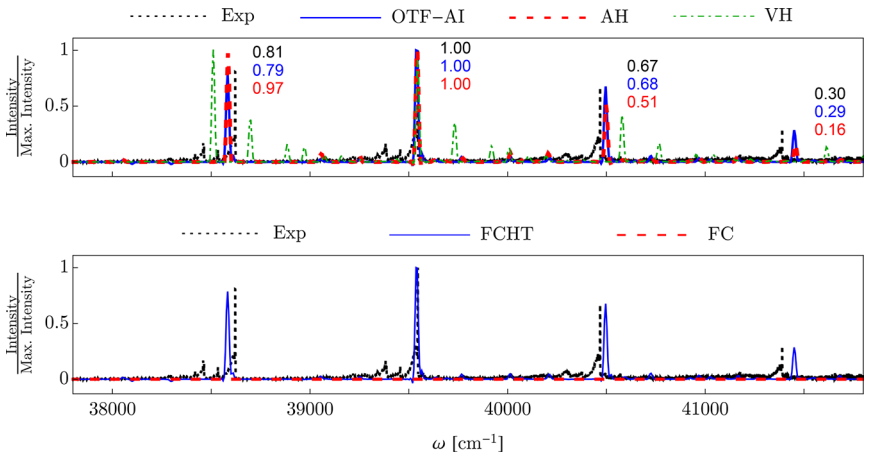

Figure 2. Calculated absorption spectra of the benzene $\tilde{A}^1B_{2u} \leftarrow \tilde{X}^1A_{1g}$ electronic transition compared to the experimental[42,43] spectrum measured at 293 K. See the caption of Figure 1 for details. To clarify the difference between the AH and OTF-AI spectra, we show the scaled intensities of the experimental (black), OTF-AI (blue), and AH (red) peaks.

reproduces the experimental spectrum rather well and with minimum human input.

To assess the validity of the Condon approximation, the FC spectra (using the Condon approximation) and Franck−Condon Herzberg−Teller (FCHT) spectra (based on the Herzberg-Teller approximation, eq 5) of the phenyl radical are compared at the bottom of Figure 1. The FC and FCHT spectra are very similar because the absorption spectrum of the phenyl radical is mostly determined by the symmetry-allowed FC transition, while the HT contribution only broadens the peaks slightly. We find that in the phenyl radical including anharmonicity effects with the OTF-AI scheme is more important than including the HT contribution with extension of the TGA.

Both the ground- and excited-state geometries of benzene belong to the D_{6h} point group. Group theory predicts that the $\tilde{A}^1B_{2u} \leftarrow \tilde{X}^1A_{1g}$ electronic transition is symmetry-forbidden. Yet, it is vibronically allowed, since the nonzero elements of the gradient of the transition dipole moment give rise to the vibronic spectrum.[28] The gradient of the transition dipole moment originates mostly from nonadiabatic couplings between the B_{2u} state and the bright E_{1u} state.[39] The spectrum contains one strong progression, assigned to one of the totally symmetric modes, as well as a number of hot bands. At present, we do not attempt to simulate the hot bands, which require finite-temperature treatment;[40] our goal is computing the correct absorption cross sections of the main progression. In addition, we do not treat the spectral features arising from the second-order vibronic coupling, i.e., a number of small-intensity peaks that cannot be described within the first-order HT approximation.[41]

Interestingly, the AH approach again reproduces the experimental spectrum at least qualitatively, unlike the vertical harmonic approach, which results in a number of peaks not observed in the experiment (Figure 2, top). In the VH model, modes 25, 29, and 30 are more distorted because their frequencies are significantly lower than the corresponding frequencies in the AH model (see Table S6 and Figure S5 of the Supporting Information). Again, due to a partial treatment of anharmonicity, the OTF-AI-ETGA spectrum shows significant improvement over both global harmonic methods. While the relative intensities of AH peaks have errors of 20−50% and the VH model fails completely, the relative intensities of the OTF-AI-ETGA peaks lie within 5% of experiment. The influence of anharmonicity on the spectrum is investigated using the autocorrelation functions in Supporting Information (see Figures S6−S8). To further explore whether it is the error in the phase or magnitude of the autocorrelation function that affects the spectra more, we construct two hybrid, nonphysical autocorrelation functions. The first, denoted |AH|exp(i OTF), combines the magnitude of the AH autocorrelation function with the phase from the on-the-fly correlation function, while the second, denoted |OTF|exp(i AH), combines the magnitude of the on-the-fly autocorrelation function with the phase from the AH autocorrelation function. The spectra in Figure 3 simulated using these two hybrid autocorrelations show clearly that it is the error in the phase of the AH model that most corrupts the intensities of the peaks. The difference between the two phases is closely related to the propagation of the stability matrix and, consequently, to the Hessians of the excited electronic state potential.

In contrast to the almost perfect description of the intensities by OTF-AI-ETGA, neither AH nor OTF-AI-ETGA reproduces correctly the experimental spacing of the peaks in the main progression. This error, however, can be assigned to the electronic structure method, implying that the use of other density functional or wave function-based methods could give more accurate curvature of the potential and hence a better spacing.

Our main result is contained in the bottom panel of Figure 2, which compares the FC spectrum (based on the Condon approximation), which can be evaluated with the original TGA, and the FCHT spectrum (based on the HT approximation, eq 5), which requires the extended TGA. While FCHT agrees very well with experiment, the FC spectrum is zero because the transition dipole moment at the ground-state equilibrium is zero, which is the precise meaning of an electronically forbidden transition.

Incidentally, one can imagine simulating the FC spectrum by the commonly adopted procedure in which the transition dipole moment is set to unity and the spectrum is rescaled at the end. Although reasonable for electronically allowed transitions, here this "blind" procedure makes no sense because $\mu_{FC} = 0$. This "FC" approach is compared to the FCHT result (see Figure S9 of the Supporting Information), and, somewhat surprisingly, the spectra are very similar, the main difference

DOI: 10.1021/acs.jpclett.8b00827
J. Phys. Chem. Lett. 2018, 9, 2367−2372

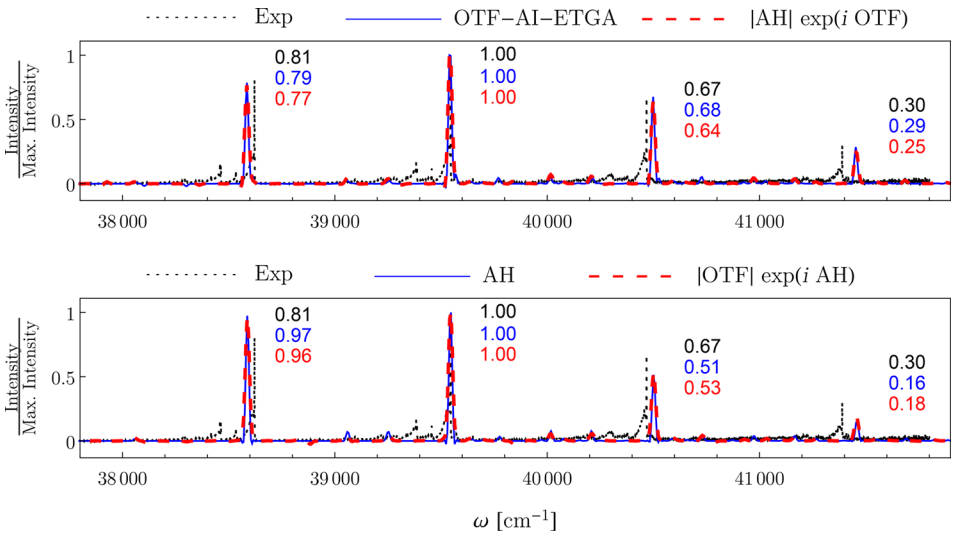

Figure 3. Spectra calculated from the hybrid autocorrelation functions: the |AH|exp(i OTF) spectrum is almost the same as the very accurate OTF-AI-ETGA spectrum (top), while the |OTF|exp(i AH) spectrum overlaps with the less accurate AH spectrum (bottom), confirming that the error in the phase of the autocorrelation function is more important than the error in its magnitude (see Table S7 of the Supporting Information). Scaled peak intensities are shown as in Figure 2.

being a constant shift corresponding exactly to the excited-state frequency of the degenerate inducing modes 27 and 28 (see Tables S5−S6 of the Supporting Information). However, such similarity between the "FC" and the FCHT approach is not general. In addition, the "FC" approach is not capable of reproducing the *absolute* magnitudes of absorption cross sections, while the full FCHT approach provides a good estimate of the absolute absorption cross sections, as shown in Figure S10 of the Supporting Information.

To conclude, we presented an extension to OTF-AI-TGA and employed it to evaluate absorption spectra of the phenyl radical and benzene within the HT approximation. Considerable improvement compared to the usual global harmonic approaches was achieved, and further insight into the origins of the spectral features was given. The results obtained for the absorption spectrum of the phenyl radical imply that including the anharmonicity effects is more important than the HT contribution to the spectrum. Although TGA is often described in the context of calculating low-resolution spectra, here we reported the evaluation of a rather high resolution absorption spectrum of benzene with high accuracy. The improvement was especially pronounced in the intensities of the peaks due to partial inclusion of the anharmonicity of the excited-state potential. Thus, OTF-AI-ETGA can be used not only to reproduce spectra but also to evaluate the importance of different effects by going beyond the commonly used Condon and global harmonic approximations.

■ ASSOCIATED CONTENT

Supporting Information

The Supporting Information is available free of charge on the ACS Publications website at DOI: 10.1021/acs.jpclett.8b00827.

Computational details, ground- and excited-state optimized geometries, transition dipole moments, frequencies, and displacements, validation of the Born−Oppenheimer approximation and of the choice of the electronic structure method, conservation of the phase space volume and symplectic structure, details of spectra calculations, models describing the failure of the vertical harmonic method for absorption spectra, discussion of anharmonicity effects in benzene, Franck−Condon spectrum, and absolute absorption cross sections of benzene (PDF)

■ AUTHOR INFORMATION

Corresponding Author

*E-mail: jiri.vanicek@epfl.ch.

ORCID

Jiří Vaníček: 0000-0002-2080-4378

Author Contributions

†These authors contributed equally to this work.

Notes

The authors declare no competing financial interest.

■ ACKNOWLEDGMENTS

The authors acknowledge financial support from the Swiss National Science Foundation through the NCCR MUST (Molecular Ultrafast Science and Technology) Network, from the European Research Council (ERC) under the European Union's Horizon 2020 research and innovation programme (Grant Agreement No. 683069 − MOLEQULE), from the COST action MOLIM (Molecules in Motion), and from the EPFL.

■ REFERENCES

(1) Herzberg, G. *Atomic Spectra and Atomic Structure*; Dover Publications, 1944.

(2) Albini, A.; Fasani, E. Introduction and Review of the Year 2015. *Photochemistry* **2016**, *44*, 1−15.

(3) Heller, E. J. The Semiclassical Way to Molecular Spectroscopy. *Acc. Chem. Res.* **1981**, *14*, 368−375.

(4) Condon, E. A Theory of Intensity Distribution in Band Systems. *Phys. Rev.* **1926**, *28*, 1182−1201.

(5) Franck, J.; Dymond, E. G. Elementary Processes of Photochemical Reactions. *Trans. Faraday Soc.* **1926**, *21*, 536−542.

(6) Meyer, H.-D.; Gatti, F.; Worth, G. A. *Multidimensional Quantum Dynamics: MCTDH Theory and Applications*; WILEY-VCH, 2009.

DOI: 10.1021/acs.jpclett.8b00827
J. Phys. Chem. Lett. 2018, 9, 2367−2372

(7) Gatti, F. *Molecular Quantum Dynamics - From Theory to Applications*; Springer-Verlag, 2014.
(8) Miller, W. H. Classical S Matrix: Numerical Application to Inelastic Collisions. *J. Chem. Phys.* **1970**, *53*, 3578.
(9) Heller, E. J. Time-dependent Approach to Semiclassical Dynamics. *J. Chem. Phys.* **1975**, *62*, 1544−1555.
(10) Heller, E. J. Frozen Gaussians: A Very Simple Semiclassical Approximation. *J. Chem. Phys.* **1981**, *75*, 2923−2931.
(11) Herman, M. F.; Kluk, E. A Semiclasical Justification for the Use of Non-spreading Wavepackets in Dynamics Calculations. *Chem. Phys.* **1984**, *91*, 27−34.
(12) Kay, K. G. Semiclassical Initial Value Treatments of Atoms and Molecules. *Annu. Rev. Phys. Chem.* **2005**, *56*, 255−280.
(13) Ben-Nun, M.; Quenneville, J.; Martínez, T. J. Ab Initio Multiple Spawning: Photochemistry from First Principles Quantum Molecular Dynamics. *J. Phys. Chem. A* **2000**, *104*, 5161−5175.
(14) Saita, K.; Shalashilin, D. V. On-the-fly ab initio molecular dynamics with multiconfigurational Ehrenfest method. *J. Chem. Phys.* **2012**, *137*, 22A506.
(15) Richings, G.; Polyak, I.; Spinlove, K.; Worth, G.; Burghardt, I.; Lasorne, B. Quantum Dynamics Simulations Using Gaussian Wavepackets: the vMCG Method. *Int. Rev. Phys. Chem.* **2015**, *34*, 269−308.
(16) Tatchen, J.; Pollak, E. Semiclassical On-the-fly Computation of the $S_0 \rightarrow S_1$ Absorption Spectrum of Formaldehyde. *J. Chem. Phys.* **2009**, *130*, 041103.
(17) Ceotto, M.; Atahan, S.; Shim, S.; Tantardini, G. F.; Aspuru-Guzik, A. First-principles Semiclassical Initial Value Representation Molecular Dynamics. *Phys. Chem. Chem. Phys.* **2009**, *11*, 3861−3867.
(18) Ceotto, M.; Atahan, S.; Tantardini, G. F.; Aspuru-Guzik, A. Multiple Coherent States for First-principles Semiclassical Initial Value Representation Molecular Dynamics. *J. Chem. Phys.* **2009**, *130*, 234113.
(19) Wong, S. Y. Y.; Benoit, D. M.; Lewerenz, M.; Brown, A.; Roy, P.-N. Determination of Molecular Vibrational State Energies Using the Ab Initio Semiclassical Initial Value Representation: Application to Formaldehyde. *J. Chem. Phys.* **2011**, *134*, 094110.
(20) Ianconescu, R.; Tatchen, J.; Pollak, E. On-the-fly Semiclassical Study of Internal Conversion Rates of Formaldehyde. *J. Chem. Phys.* **2013**, *139*, 154311.
(21) Gabas, F.; Conte, R.; Ceotto, M. On-the-fly Ab Initio Semiclassical Calculation of Glycine Vibrational Spectrum. *J. Chem. Theory Comput.* **2017**, *13*, 2378.
(22) Grossmann, F. A Semiclassical Hybrid Approach to Many Particle Quantum Dynamics. *J. Chem. Phys.* **2006**, *125*, 014111.
(23) Wehrle, M.; Šulc, M.; Vaníček, J. On-the-fly Ab Initio Semiclassical Dynamics: Identifying Degrees of Freedom Essential for Emission Spectra of Oligothiophenes. *J. Chem. Phys.* **2014**, *140*, 244114.
(24) Wehrle, M.; Oberli, S.; Vaníček, J. On-the-fly Ab Initio Semiclassical Dynamics of Floppy Molecules: Absorption and Photoelectron Spectra of Ammonia. *J. Phys. Chem. A* **2015**, *119*, 5685.
(25) Herzberg, G.; Teller, E. Schwingungsstruktur der Elektronenübergänge Bei Mehratomigen Molekülen. *Z. Phys. Chem.* **1933**, *21*, 410.
(26) Lee, S.-Y.; Heller, E. J. Exact Time-dependent Wave Packet Propagation: Application to the Photodissociation of Methyl Iodide. *J. Chem. Phys.* **1982**, *76*, 3035−3044.
(27) Biczysko, M.; Bloino, J.; Barone, V. First Principle Simulation of Vibrationally Resolved $\tilde{A}^2B_1 \leftarrow \tilde{X}^2A_1$ Electronic Transition of Phenyl Radical. *Chem. Phys. Lett.* **2009**, *471*, 143−147.
(28) Herzberg, G. *Molecular Spectra and Molecular Structure: III. Electronic Spectra of Polyatomic Molecules*; D. Van Nostrand Company Inc., 1966.
(29) Hein, B.; Kreisbeck, C.; Kramer, T.; Rodríguez, M. Modelling of oscillations in two-dimensional echo-spectra of the Fenna-Matthews-Olson complex. *New J. Phys.* **2012**, *14*, 023018.
(30) Begušić, T.; Patoz, A.; Vaníček, J. *In preparation*.
(31) Quack, M.; Merkt, F. *Handbook of High-resolution Spectroscopy*; John Wiley & Sons, 2011.
(32) Domcke, W.; Cederbaum, L. S.; Köppel, H.; VonNiessen, W. A Comparison of Different Approaches to the Calculation of Franck-Condon Factors for Polyatomic Molecules. *Mol. Phys.* **1977**, *34*, 1759−1770.
(33) Baiardi, A.; Bloino, J.; Barone, V. General Time Dependent Approach to Vibronic Spectroscopy Including Franck-Condon, Herzberg-Teller, and Duschinsky Effects. *J. Chem. Theory Comput.* **2013**, *9*, 4097−4115.
(34) Duschinsky, F. On the Interpretation of Electronic Spectra of Polyatomic Molecules. *Acta Physicochim. U.R.S.S.* **1937**, *7*, 551−566.
(35) Cerezo, J.; Zuniga, J.; Requena, A.; Ávila Ferrer, F. J.; Santoro, F. Harmonic Models in Cartesian and Internal Coordinates to Simulate the Absorption Spectra of Carotenoids at Finite Temperatures. *J. Chem. Theory Comput.* **2013**, *9*, 4947−4958.
(36) Tannor, D. J. *Introduction to Quantum Mechanics*; University Science Books, 2007.
(37) Tutt, L. W.; Zink, J. I.; Heller, E. J. Simplifying the MIME: A Formula Relating Normal Mode Distortions and Frequencies to the MIME Frequency. *Inorg. Chem.* **1987**, *26*, 2158−2160.
(38) Radziszewski, J. Electronic Absorption Spectrum of Phenyl Radical. *Chem. Phys. Lett.* **1999**, *301*, 565−570.
(39) Li, J.; Lin, C.-K.; Li, X. Y.; Zhu, C. Y.; Lin, S. H. Symmetry Forbidden Vibronic Spectra and Internal Conversion in Benzene. *Phys. Chem. Chem. Phys.* **2010**, *12*, 14967−76.
(40) He, Y.; Pollak, E. Theory of Cooling of Room Temperature Benzene upon Photo-Excitation to the S1 State. *J. Phys. Chem. A* **2001**, *105*, 10961−10966.
(41) Fischer, G.; Reimers, J.; Ross, I. CNDO-calculation of second order vibronic coupling in the $1B_{2u} - 1A_{1g}$ transition of benzene. *Chem. Phys.* **1981**, *62*, 187−193.
(42) Fally, S.; Carleer, M.; Vandaele, A. C. UV Fourier Transform Absorption Cross Sections of Benzene, Toluene, Meta-, Ortho-, and Para-Xylene. *J. Quant. Spectrosc. Radiat. Transfer* **2009**, *110*, 766−782.
(43) Keller-Rudek, H.; Moortgat, G. K.; Sander, R.; Sörensen, R. The MPI-Mainz UV/VIS Spectral Atlas of Gaseous Molecules of Atmospheric Interest. *Earth Syst. Sci. Data* **2013**, *5*, 365−373.

DOI: 10.1021/acs.jpclett.8b00827
J. Phys. Chem. Lett. 2018, 9, 2367−2372